# Neuroprotection against Traumatic Brain Injury by Xenon, but Not Argon, Is Mediated by Inhibition at the *N*-Methyl-D-Aspartate Receptor Glycine Site

Katie Harris, B.Sc.,* Scott P. Armstrong, M.Sc.,* Rita Campos-Pires, M.D.,* Louise Kiru, M.Res.,† Nicholas P. Franks, F.R.C.A., F.Med.Sci., F.R.S.,‡ Robert Dickinson, Ph.D.§

## ABSTRACT

**Background:** Xenon, the inert anesthetic gas, is neuroprotective in models of brain injury. The authors investigate the neuroprotective mechanisms of the inert gases such as xenon, argon, krypton, neon, and helium in an *in vitro* model of traumatic brain injury.

**Methods:** The authors use an *in vitro* model using mouse organotypic hippocampal brain slices, subjected to a focal mechanical trauma, with injury quantified by propidium iodide fluorescence. Patch clamp electrophysiology is used to investigate the effect of the inert gases on *N*-methyl-D-aspartate receptors and TREK-1 channels, two molecular targets likely to play a role in neuroprotection.

**Results:** Xenon (50%) and, to a lesser extent, argon (50%) are neuroprotective against traumatic injury when applied after injury (xenon 43 ± 1% protection at 72 h after injury [N = 104]; argon 30 ± 6% protection [N = 44]; mean ± SEM). Helium, neon, and krypton are devoid of neuroprotective effect. Xenon (50%) prevents development of secondary injury up to 48 h after trauma. Argon (50%) attenuates secondary injury, but is less effective than xenon (xenon 50 ± 5% reduction in secondary injury at 72 h after injury [N = 104]; argon 34 ± 8% reduction [N = 44]; mean ± SEM). Glycine reverses the neuroprotective effect of xenon, but not argon, consistent with competitive inhibition at the *N*-methyl-D-aspartate receptor glycine site mediating xenon neuroprotection against traumatic brain injury. Xenon inhibits *N*-methyl-D-aspartate receptors and activates TREK-1 channels, whereas argon, krypton, neon, and helium have no effect on these ion channels.

**Conclusions:** Xenon neuroprotection against traumatic brain injury can be reversed by increasing the glycine concentration, consistent with inhibition at the *N*-methyl-D-aspartate receptor glycine site playing a significant role in xenon neuroprotection. Argon and xenon do not act *via* the same mechanism.

### What We Already Know about This Topic

- Xenon has been shown to be neuroprotective in ischemic brain injury models
- The cellular mechanisms of this effect are not well understood

### What This Article Tells Us That Is New

- Given after traumatic injury to hippocampal slices, xenon (and argon to a lesser degree) halves the secondary neuronal injury
- *N*-methyl-D-aspartate antagonism is an important component of this protective effect

TRAUMATIC brain injury (TBI) is a major cause of death and disability throughout the world. In developed countries, TBI is the main cause of death and disability in those who are aged less than 45 yr[1] with falls and motor vehicle crashes being the leading causes.[2] Currently, there are no treatments aimed specifically at preventing neuronal loss after TBI.[3–5] TBI is characterized by a "primary injury" determined by the initial mechanical force, followed by a "secondary injury" developing hours to days after the initial trauma. Secondary injury is thought to underlie the majority of the short- and long-term neurological and cognitive impairments that follow TBI,[6–8] hence treatments to prevent or limit secondary injury are of clinical importance. The pathophysiology of secondary injury is complex, involving

* Ph.D. Student, † Masters Student, ‡ Professor of Biophysics and Anaesthetics, § Lecturer in Anaesthetics, Anaesthetics, Pain Medicine, and Intensive Care Section, Department of Surgery and Cancer, Biophysics Section, Imperial College London, London, United Kingdom.

Received from Anaesthetics, Pain Medicine & Intensive Care Section, Department of Surgery & Cancer, Imperial College London, London, United Kingdom. Submitted for publication February 22, 2013. Accepted for publication June 20, 2013. Support was provided by the European Society for Anaesthesiology, Brussels, Belgium; The Royal College of Anaesthetists, London, United Kingdom; and Westminster Medical School Research Trust, London, United Kingdom. Katie Harris is the recipient of a studentship from the Westminster Medical School Research Trust, London, United Kingdom. Scott Armstrong is the recipient of a studentship from the Medical Research Council, London, United Kingdom. Dr. Campos-Pires is the recipient of a doctoral training award from the Fundação para a Ciência e a Tecnologia, Lisbon, Portugal. Professor Franks has a financial interest in the use of xenon as a neuroprotectant, through an agreement with Air Products and Chemicals, Inc., Allentown, Pennsylvania.

Address correspondence to Dr. Dickinson: Sir Ernst Chain Building, Imperial College London, South Kensington, London SW7 2AZ, United Kingdom. r.dickinson@imperial.ac.uk. Information on purchasing reprints may be found at www.anesthesiology.org or on the masthead page at the beginning of this issue. ANESTHESIOLOGY's articles are made freely accessible to all readers, for personal use only, 6 months from the cover date of the issue.

 Anesthesiology 2013; 119:1137-48

multiple injury cascades,[9,10] but glutamate excitotoxicity is believed to play a key role.[11–13]

The anesthetic noble gas xenon inhibits the *N*-methyl-D-aspartate (NMDA)-subtype of glutamate receptor and has been shown to be neuroprotective in models of brain injury.[14–24] In this article, we test the hypothesis that, in addition to xenon, other noble gases are neuroprotective in an *in vitro* model of TBI. After the finding that xenon protects against ischemic injury, other noble gases have been investigated as potential neuroprotectants in models of ischemia.[25–27] Argon has been found to be protective in *in vivo* and *in vitro* models of ischemia,[27–30] however, a recent study reported a protective effect of argon *in vitro* but no effect *in vivo*.[31] The situation with the other noble gases is even less clear. Some studies report helium is neuroprotective against ischemia,[19,32,33] whereas others find no effect.[34] Another study found that helium, neon, and krypton were actually detrimental in ischemic injury.[35] In traumatic injury, the potential protective effect of the noble gases has been less well studied, but xenon, helium, and argon are reported to be protective in *in vitro* models of trauma.[19,28] However, to date, there have been no studies systematically investigating the complete series of noble gases under identical conditions in a model of trauma. Furthermore, there have been few studies that have investigated the effects of inert gases (except xenon) on molecular targets that may be involved in neuroprotection[26] such as NMDA receptors and two-pore domain potassium channels.

We recently showed that the mechanism of xenon protection against ischemic injury is mediated by inhibition at the NMDA receptor glycine site.[34] In this study, we test the hypothesis that xenon's protective effect against TBI is mediated by inhibition at the NMDA receptor glycine-binding site. We also test the hypothesis that xenon and other neuroprotective inert gases act *via* the same mechanism. We discovered that xenon is an NMDA receptor antagonist and that it acts by competing with the coagonist glycine.[36–38] This means that xenon inhibits NMDA receptors less at higher glycine concentrations.[37] This property can be used as a pharmacological tool to investigate the mechanism of xenon neuroprotection. If xenon neuroprotection can be reversed by increased glycine concentration, this is consistent with the effect being due to NMDA receptor glycine site inhibition.[34]

## Materials and Methods

### Hippocampal Organotypic Slices

All experiments were performed in compliance with the United Kingdom Animals (Scientific Procedures) Act of 1986 and the Ethical Review Committee of Imperial College London, London, United Kingdom. All efforts were made to minimize animal suffering and the number of animals used. Unless otherwise stated, chemicals were obtained from Sigma Chemical Company Ltd. (Poole, Dorset, United Kingdom). Organotypic hippocampal slice cultures were prepared as previously described[39] with some modifications. In brief, 6-day-old C57BL/6 mouse pups (Harlan Ltd., Bicester, Oxfordshire, United Kingdom) were humanely killed by cervical dislocation, brains were removed and placed in ice-cold "preparation" medium. The preparation medium contained Gey balanced salt solution, 5 mg/ml of D-glucose, and 1% antibiotic–antimycotic suspension. The hippocampi were removed from the brains and 400-μm thick transverse slices were prepared using a Mcllwain tissue chopper (Mickle Laboratory Engineering Co., Guildford, Surrey, United Kingdom). Slices were transferred into ice-cold preparation medium, gently separated under a stereomicroscope, and then placed onto tissue-culture inserts (Millicell-CM; Millipore Corporation, Carrigtwohill, Co., Cork, Ireland) that were inserted into 35-mm Petri dishes. The wells contained "growth" medium, which consisted of 50% Eagle minimal essential media, 25% Hank balanced salt solution, 25% inactivated horse serum, 3 mM of L-glutamine, 5 mg/ml of D-glucose, 1% antibiotic–antimycotic suspension, and 10 mM of HEPES titrated to pH 7.2. Slices were incubated at 37°C in a 95% air–5% $CO_2$ humidified atmosphere. The growth medium was changed every 3 days. Experiments were carried out after 12 days in culture.

### Traumatic Injury and Hyperbaric Gas Chamber

After the hippocampal slices had been in culture for 12 days, the inserts were transferred to six-well tissue-culture plates, and the growth medium was changed to "experimental" medium. The experimental medium was serum-free and consisted of 75% Eagle minimal essential media, 25% Hank balanced salt solution, 3 mM of L-glutamine, 5 mg/ml of D-glucose, 1% antibiotic–antimycotic suspension, 4.5 μM of propidium iodide (PI), and 10 mM of HEPES titrated to pH 7.2. One hour after transfer to experimental media, the slices were imaged to assess slice viability before injury. Typically, slices exhibited very little PI fluorescence, an indicator of tissue health. A small number of slices showed regions of dense staining, indicating compromised viability, presumably due to mechanical damage during the slice preparation stage. These slices were excluded from further analysis. One hour after imaging, slices were subjected to traumatic injury. The trauma was produced with a specially designed apparatus based on published descriptions.[19,40] Under a stereomicroscope, a stylus was positioned above the CA1 region of the hippocampus using a three-axis micromanipulator. The stylus dropped onto the slice when power to a small electromagnet was switched off. The distal part of the stylus was smooth and rounded to prevent perforation of the slice and the impact produced a focal injury with a diameter of 340 ± 12 μm (N = 50 slices).

After traumatizing the CA1 region, the culture plates were immediately transferred to a small pressure chamber,[34] which contained a high-speed fan for rapid gas mixing, housed in an incubator set at 37°C. The chamber (gas volume 0.925 l) was flushed with humidified control gas (75% nitrogen–20%

oxygen–5% $CO_2$) for 5 min at 5 l/min, which would ensure better than 99.99% gas replacement. After flushing, the pressure chamber was sealed and 0.5 atm of noble gas was added, giving a total pressure of 1.5 atm. After a given time in the chamber (30 min to 24 h), the slices were imaged using a fluorescent microscope (see Quantifying Cell Injury). It was previously shown that uptake of PI by slices is complete within 30 min.[19] After completing the imaging, the slices were transferred back to the pressure chamber and the appropriate gas mixture reestablished. This procedure was repeated at 48 and 72 h after trauma. Note that, for all gas mixtures and for all pressures, the partial pressures of oxygen and carbon dioxide were fixed at 0.2 and 0.05 atm, respectively.

### Quantifying Cell Injury

PI is a membrane-impermeable dye that only enters cells with damaged cell membranes.[41] Inside the cells, it binds principally to DNA and becomes highly fluorescent, with a peak emission spectrum in the red region of the visible spectrum. An epi-illumination microscope (Nikon Eclipse 80; Kingston upon Thames, Surrey, United Kingdom) with a low-power (×2) objective was used to visualize the PI fluorescence. A digital video camera and software (Micropublisher 3.3 RTV camera and QCapture Pro software; Qimaging Inc., Surrey, British Columbia, Canada) were used to capture the images. The images were analyzed using ImageJ software.‖ Red, green, and blue channels were recorded, but only the red channel was used and the distribution of intensities was plotted as a histogram with 256 intensity levels. Slices under standard control conditions (incubated in the chamber for 72 h at 37°C with 95% air and 5% $CO_2$) showed a well-defined peak in the intensity distribution which fell rapidly to zero. In contrast, after trauma, the peak in the intensity distribution was lower, broader, and shifted to higher intensity levels. As a measure of trauma, we integrated the number of pixels above a threshold of 50, which under our experimental conditions provided a robust quantitative measurement of PI fluorescence, and hence of cell injury.[34] Because the light output from the mercury lamp changed over time, the exposure time was adjusted to take this into account. This was done by recording fluorescence from a glass slide standard (Fluor-Ref; Omega Optical, Brattleboro, VT) and adjusting the exposure time accordingly.

### Electrophysiology

Human embryonic kidney, cells (tsA201) were plated on glass coverslips and transfected with complementary DNA for rat NMDA receptor GluN1-1a and GluN2A receptors or human TREK-1 channels and green fluorescent protein for identification, as described previously.[38,42] Whole-cell recordings were made using an Axoclamp 200B amplifier (Axon Instruments, Foster City, CA). Pipettes (3–5 MΩ) were fabricated from borosilicate glass. For NMDA receptor experiments, internal solution contained 110 mM of K-gluconate, 2.5 mM of NaCl, 10 mM of HEPES, 10 mM of 1,2-Bis(2-aminophenoxy)ethane-*N*,*N*,*N*′,*N*′-tetraacetic acid, titrated to pH 7.3 using KOH, and the extracellular solution contained: 150 mM of NaCl, 2.5 mM of KCl, 2 mM of $CaCl_2$, 10 mM of HEPES, titrated to pH 7.35 using NaOH. Cells were voltage clamped at −60 mV. For TREK-1 experiments, the intracellular solution contained 120 mM of $KCH_3SO_4$, 4 mM of NaCl, 1 mM of $MgCl_2$, 1 mM of $CaCl_2$, 10 mM of EGTA, 10 mM of HEPES, 3 mM of MgATP, and 0.3 mM of NaGTP, titrated to pH 7.3 with KOH, and the extracellular solution contained 145 mM of NaCl, 2.5 mM of KCl, 1 mM of $CaCl_2$, 2 mM of $MgCl_2$, 10 mM of HEPES, 10 mM of D-Glucose, titrated to pH 7.4 with NaOH. Cells were voltage clamped at −80 mV and voltage ramps from −120 to 0 mV and from 0 to −80 mV were performed over 250 ms. Currents were filtered at 100 Hz (−3 dB) using an eight-pole Bessel filter (model 900; Frequency Devices Inc., Ottawa, IL), digitized at 20 kHz (Digidata 1332A; Axon Instruments) and stored on a computer. Solutions containing the inert gases were prepared by bubbling gases through sintered glass bubblers in Dreschel bottles containing extracellular saline, as described previously.[37,43]

### Statistical Analysis

We assessed significance using two-way ANOVA, with Bonferroni *post hoc* test. Factor 1 was inert gas or treatment (He, Xe, Kr, glycine, and others) and factor 2 was the time after injury (*e.g.*, 24, 48, and 72 h). Our experimental design involved measuring the injury development over time in the same set of slices, for a given experimental condition (*e.g.*, inert gas); in most cases, these times were at 24, 48, and 72 h after injury. We, therefore, used repeated-measures ANOVA with factor 1 as the repeated factor. We used two-tailed hypothesis testing with $P$ values of less than 0.05 taken to indicate a significant difference among groups. The samples sizes (N) are indicated in the figures. For the main inert gas neuroprotection experiments, we aimed to have samples sizes of at least 30–40 slices in each group. In every experiment, the slices were imaged at 1 h before the experiment to assess slice viability before injury; a small number of slices showed regions of dense PI staining before injury indicating compromised viability presumably due to mechanical damage in the cell-culturing process. These slices were excluded from further analysis. This resulted in some groups having fewer slices than others. In the injury-development experiments (fig. 1), we wished to minimize the number of times that the slices were removed from the chamber for imaging at early time points. We, therefore, decided to limit the number of imaging sessions to four for each slice set. We used the protocol that had one imaging session at an early time point (0.5 h or 1 h or 3 h or 6 h or 12 h) followed by three further imaging sessions at 24, 48, and 72 h. We aimed to have 8–10 slices in each of the early time-point groups. This design resulted in a

‖ Available at: http://rsb.info.nih.gov. Accessed April 29, 2013.

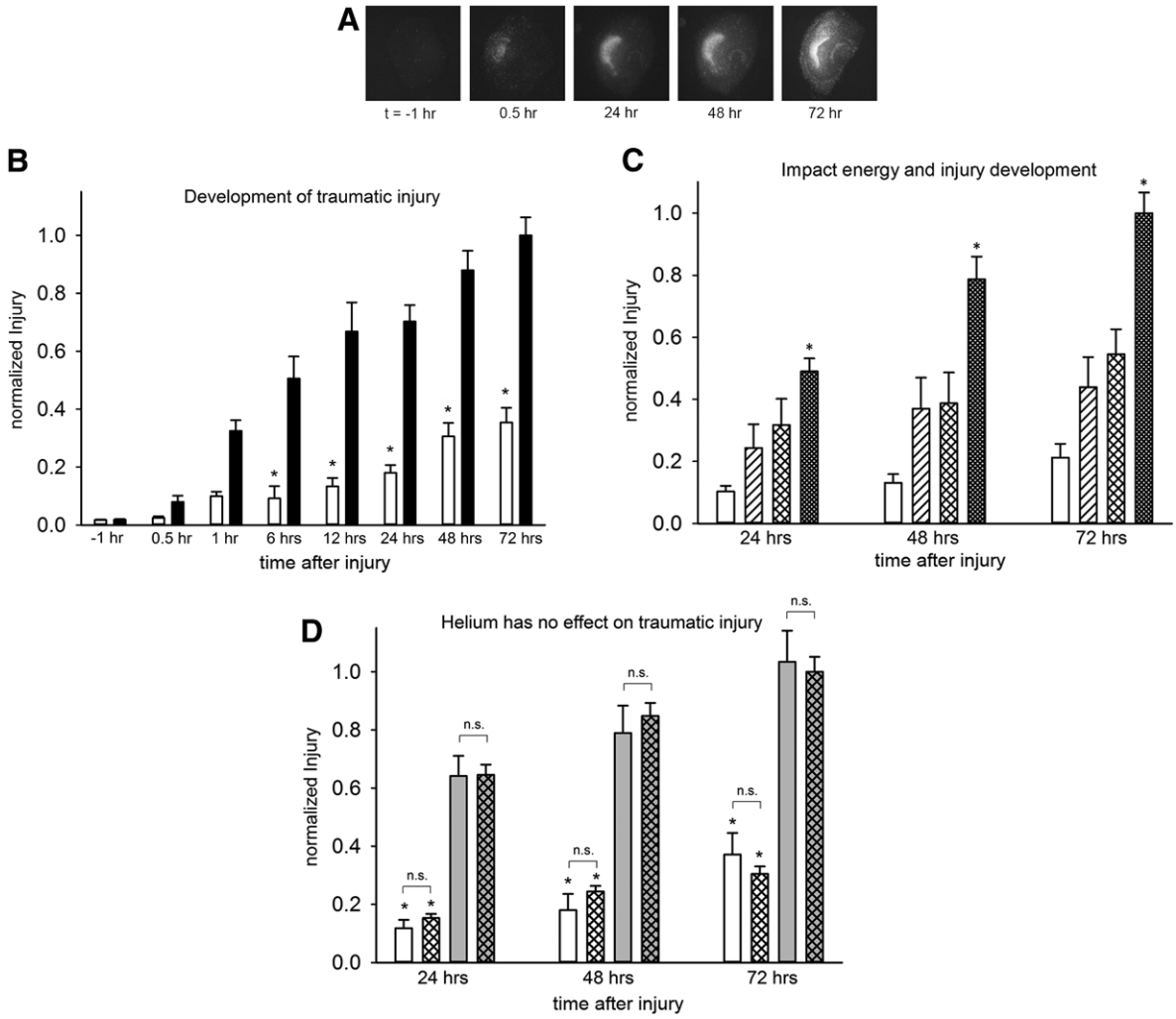


**Fig. 1.** (*A*) Propidium iodide fluorescent images of slices at 1 h before injury, and 30 min, 24 h, 48 h, and 72 h after injury. (*B*) Development of injury (*black bars*) compared to sham (*white bars*) quantified by propidium iodide fluorescence intensity, after injury with impact energy of 3.5 μJ. The *error bars* are standard errors. *Indicates value significantly different ($P < 0.05$) from injured slices at each time point (N = 48: traumatic brain injury (TBI), t = –1, 24, 48, and 72 h; N = 33: sham, t = –1, 24, 48, and 72 h; N = 5: TBI 0.5 h; N = 4: sham 0.5 h; N = 11: TBI 1 h; N = 13: sham 1 h; N = 19: TBI 6 h; N = 8: sham 6 h; N = 13: TBI 12 h; N = 8: sham 12 h). (*C*) Development of injury with different traumatic impact energies. Uninjured sham slices are shown as *white bars*, compared with injured slices with impact energies of 1.4 μJ (*hatched bars*), 2.7 μJ (*crosshatched bars*), and 3.5 μJ (*black bars*). Data have been normalized to 3.5 μJ at 72 h after injury. The *error bars* are standard errors. *Indicates value significantly different ($P < 0.05$) from sham slices at each time point (N = 33: sham; N = 43: 3.5 μJ; N = 7: 1.4 μJ, 2.7 μJ). (*D*) The addition of 0.5 atm of helium had no effect on the injured or sham-treated slices. Sham-treated slices are shown as *white bars* (no helium) or *white crosshatched bars* (helium), and injured slices are shown as *grey bars* (no helium) or *grey crosshatched bars* (helium). The *error bars* are standard errors. The data have been normalized to traumatic injury with 0.5 atm helium at 72 h after injury. *Indicates value significantly different ($P < 0.001$) from injured slices at each time point (N = 141 helium TBI; N = 105 helium sham; N = 23 no helium TBI; N = 25 no helium sham).

greater number of slices in the 24-, 48-, and 72-h groups (approximately 40 slices). Where error bars shown these are the SEM. Statistical tests were implemented using the SigmaPlot (Systat Inc., Point Richmond, CA) or Origin (OriginLab Inc., Northampton, MA) software packages. The lines shown in figure 2 were drawn by eye and have no theoretical significance. Electrophysiological data traces for TREK-1 channels in figure 5 each contain 3,000 data points (equally spaced, sampled at 20 kHz), the lines shown are through these individual points.

## Results

### *Traumatic Injury and Development of Secondary Injury*

We first investigated the development of control injury in our model (fig. 1). To determine the optimum traumatic injury, we performed a series of experiments with impact energies from 1.4 to 3.5 μJ (fig. 1C). We aimed to determine an impact energy that would produce a focal primary lesion and that exhibited a developing secondary injury. We found that an impact energy of 3.5 μJ, corresponding to a stylus drop

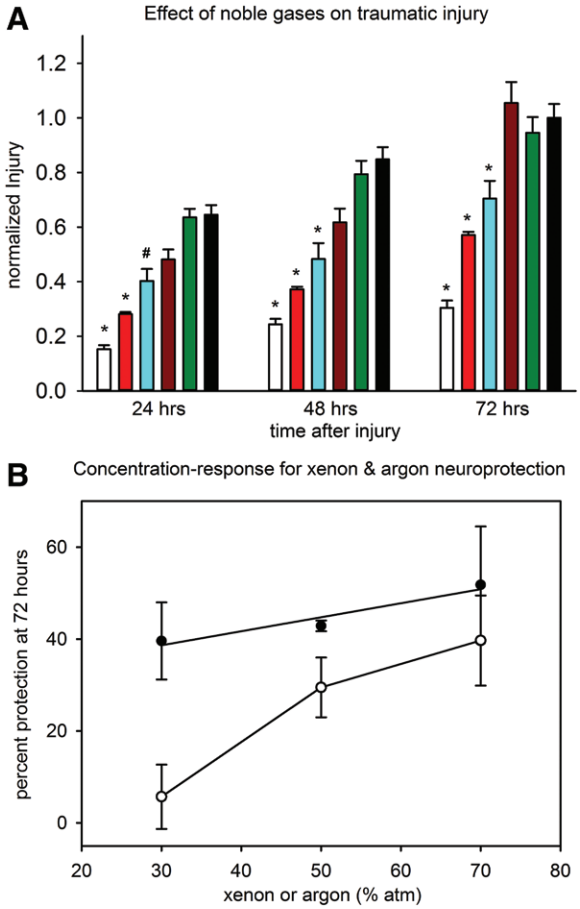


**Fig. 2.** (*A*) Effect of 50% atmosphere of the inert gases xenon (*red bars*), argon (*cyan bars*), krypton (*brown bars*), and neon (*green bars*) on control traumatic injury (*black bars*) at 24, 48, and 72 h after injury. Sham-treated slices (*white bars*) were not subject to trauma. Xenon and argon provided significant neuroprotection at all time points. Xenon was more effective than argon, with xenon-treated slices being 57 ± 1% of control injury compared with 70 ± 6% of control injury for argon-treated slices, 72 h after injury. None of the other inert gases provided significant protection against injury at any of the time points. The *error bars* are standard errors. The data have been normalized to the control injury at 72 h after injury. *Indicates value significantly different ($P < 0.001$) from control injury at each time point. #Indicates value significantly different ($P < 0.01$) from control injury (N = 141 control traumatic injury; N = 105 sham; N = 104 xenon; N = 44 argon; N = 45 krypton; N = 22 neon). (*B*) Concentration–response relationship for neuroprotection by xenon and argon. Xenon (*filled circles*) exhibited a neuroprotective effect at a concentration of 30% atm, with 40 ± 8% protection, increasing to 52 ± 13% protection at 70% atm xenon. In contrast, argon (*open circles*) was not neuroprotective at 30% atm but did exhibit a protective effect at concentrations of 50% atm and 70% atm argon. *Lines* shown were drawn by eye and have no theoretical significance. *Error bars* are standard errors (50% xenon: N = 104; 30% xenon: N = 6; 70% xenon: N = 6; 50% argon: N = 44; 30% argon: N = 14; 70% argon: N = 10).

of 5 mm, produced a consistent and reproducible focal traumatic injury that developed significantly ($P < 0.001$) over 72 h, compared with uninjured slices, and we chose 3.5 μJ as our standard injury. To determine the role of the NMDA receptor in our injury model, we performed experiments with the NMDA receptor open-channel blocker MK801. We found that 100 μM MK801 reduced injury to 37 ± 12%, 42 ± 4%, and 84 ± 7% of control at 24, 48, and 72 h after injury, respectively (N = 7; data not shown). The large reduction in injury at 24 and 48 h is consistent with a role of NMDA receptor in injury development, whereas the attenuation of the reduction at 72 h most likely reflects the intrinsic toxicity that has been reported for MK801 and other open-channel blockers such as ketamine. We wished to determine how the injury developed early after trauma with the aim of distinguishing the primary lesion and secondary injury development over time. The development of the injury was determined at time intervals from 30 min to 72 h after trauma. Figure 1A shows images of slices 1 h before injury and 30 min, 24 h, 48 h, and 72 h after traumatic injury. In these experiments, we limited the number of imaging sessions for a given slice set to four (to avoid having slices out of the stable temperature and humidity of the chamber for extended periods). Figure 1B shows the development of the injury from 30 min to 72 h after trauma. The earliest time point that we could observe injury compared with sham slices was 30 min after impact. At this point, injury was 8 ± 2% of total injury at 72 h, whereas sham slices not subjected to injury had a barely measurable PI fluorescence. We took this 30-min point as a measure of the "primary injury" in our model. Secondary injury began to develop early in this model. By 1 h after trauma, the injury had developed to 32 ± 4% of total and by 6 h the injury development was 51 ± 8% of the total injury, increasing at 12 h to 67 ± 10% of the total injury present at 72 h.

Because the neuroprotection experiments would use 0.5 atm of noble gases, we determined whether pressure *per se* would affect the injury. The effect of 0.5 atm helium on both sham-treated and trauma-injured slices was investigated (fig. 1D). Helium was chosen because it is unlikely to exert any pharmacologic effect of its own at these low pressures and any effect observed can be attributed to the effect of pressure alone. Figure 1D shows that 0.5 atm helium had no significant effect ($P > 0.3$) on either the sham- or trauma-injured slices at any time point. Nevertheless, in the experiments with xenon and the other noble gases, we used 0.5 atm helium as a control for any effect of the added pressure.

### Neuroprotection by the Noble Gases

Figure 2A shows the effect of 50% atm of xenon, argon, neon, and krypton on injury development at 24, 48, and 72 h after trauma. Xenon and argon showed a significant neuroprotection ($P < 0.01$) at each time point, but krypton, neon, and helium were without effect. Xenon potently protected against trauma, with injury in xenon-treated slices being reduced by 57 ± 3% ($P < 0.001$) compared with the untreated injured slices 24 h after injury. A similar degree of protection (56 ± 3%; $P < 0.001$) was seen 48 h after injury, whereas at 72 h after injury, the degree of protection by xenon was 43 ± 3% ($P < 0.001$). Argon was less effective than

xenon, but exhibited a similar trend, with injury in argon-treated slices being reduced by 38 ± 7% ($P < 0.01$) compared with untreated injured slices at 24 h after injury, 43 ± 7% ($P < 0.001$) at 48 h after injury and by 30 ± 7% ($P < 0.001$) at 72 h after injury. We further investigated the relative efficacy of xenon and argon by determining the concentration–response of these two inert gases (fig. 2B). Xenon was more effective than argon at all concentrations. At a concentration of 30% atm, xenon provided protection of 40 ± 8%, whereas argon was without protective effect (6 ± 7%) at the same concentration. At 50% atm, xenon provided 43 ± 3% protection, whereas argon provided 30 ± 7% protection, and at 70% atm, xenon provided protection of 52 ± 13%, whereas argon protected by 40 ± 10%.

### Xenon and Argon Reduce Secondary Injury Development

To understand the mechanism of action of xenon and argon, we determined the effect of these gases on secondary injury development (fig. 3), calculated by subtracting the primary injury measured at 30 min after trauma. Xenon was particularly effective at preventing development of the secondary injury. At 24 h after injury, xenon-treated slices were almost identical to uninjured sham slices, with injury of 14 ± 2% and 15 ± 1% of the total injury at 72 h in xenon-treated and sham slices, respectively (fig. 3A). The same was true at 48 h with xenon-treated slices 23 ± 2% of total injury compared with uninjured sham slices 24 ± 2% of total injury. At 72 h after trauma, xenon-treated slices exhibited greater injury (43 ± 4%) compared with uninjured sham slices (30 ± 3%), but this difference was not significant ($P > 0.8$). Compared with untreated injured slices, xenon reduced secondary injury by 50 ± 3% at 72 h, and this was highly significant ($P < 0.001$). Argon attenuated secondary injury, but was less effective than xenon (fig. 3B), reducing secondary injury significantly by 48 ± 9% ($P < 0.01$) at 24 h, 51 ± 7% ($P < 0.001$) at 48 h, and by 34 ± 8% ($P < 0.001$) at 72 h after injury.

### Mechanism of Neuroprotection by Xenon and Argon

To test the hypothesis that xenon neuroprotection is mediated by competitive inhibition at the NMDA receptor glycine site, we performed experiments where we investigated whether increased glycine concentration could reverse xenon's neuroprotective action. We chose to use glycine rather than serine in these experiments because we had previously established from electrophysiological experiments that glycine attenuated the effects of xenon at the NMDA receptor, and we had established accurate glycine concentration–response relationships for the GluN1/GluN2A and GluN1/GluN2B subunit combinations that predominate in the hippocampus.[37,38] We first established whether adding glycine had an effect on injury in our *in vitro* model. Figure 4A shows the effect of adding 100 μM glycine on trauma-injured or sham-treated slices. We chose a concentration of 100 μM glycine because this is a saturating concentration for the GluN1/GluN2A and GluN1/GluN2B subunit combinations.[37,38]

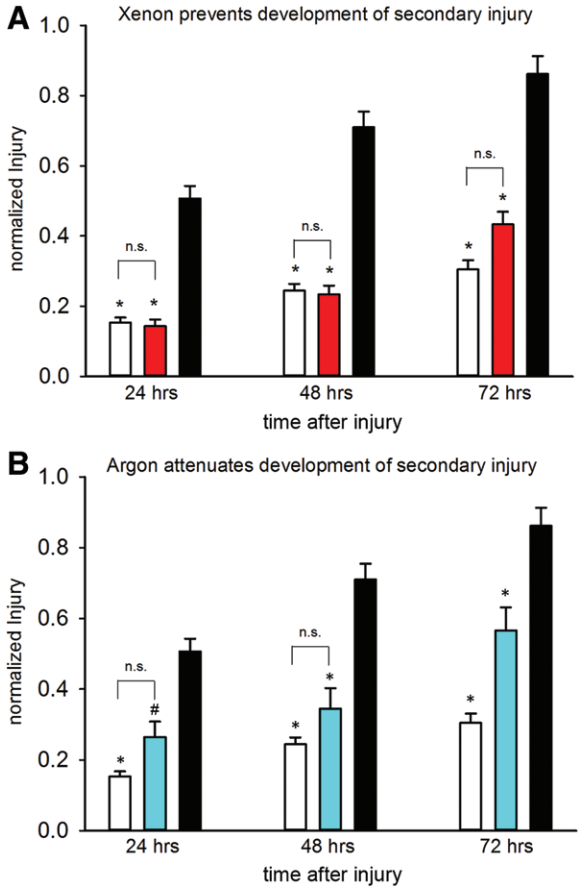


**Fig. 3.** Effect of xenon and argon on secondary injury development. (*A*) Xenon is particularly effective at preventing development of secondary injury. At the 24, 48, and 72 h time points, xenon-treated slices (*red bar*) were not significantly different to uninjured sham slices (*white bar*). At the 72-h time point, secondary injury in xenon-treated slices was 50 ± 5% of secondary injury in untreated injured slices (*black bar*). The *error bars* are standard errors. (*B*) Argon attenuates development of secondary injury at 24, 48, and 72 h after injury. At the 72-h time point, argon-treated slices (*cyan bar*) were 66 ± 8% of secondary injury in untreated injured slices (*black bar*). The *error bars* are standard errors. *Indicates value significantly different ($P < 0.001$) from control injury at each time point. #Indicates value significantly different ($P < 0.01$) from control injury (N = 141 control traumatic injury; N = 105 sham; N = 104 xenon; N = 44 argon).

We found there was no significant difference in the injured slices at 24, 48, or 72 h ($P > 0.6$) after injury in the presence of 100 μM glycine. Similarly, sham-control slices in the absence and presence of glycine were not significantly different at 24, 48, or 72 h ($P > 0.6$). To rule out a possible role of strychnine-sensitive inhibitory glycine receptors in our injury model, we tested the effect of adding 100 nM strychnine, a concentration that has been shown to abolish inhibitory glycine receptor responses at glycine concentrations up to 300 μM.[44] Strychnine had no significant effect on injured ($P > 0.6$) or sham slices ($P > 0.6$) at any time point (fig. 4A). Having established that adding glycine did not

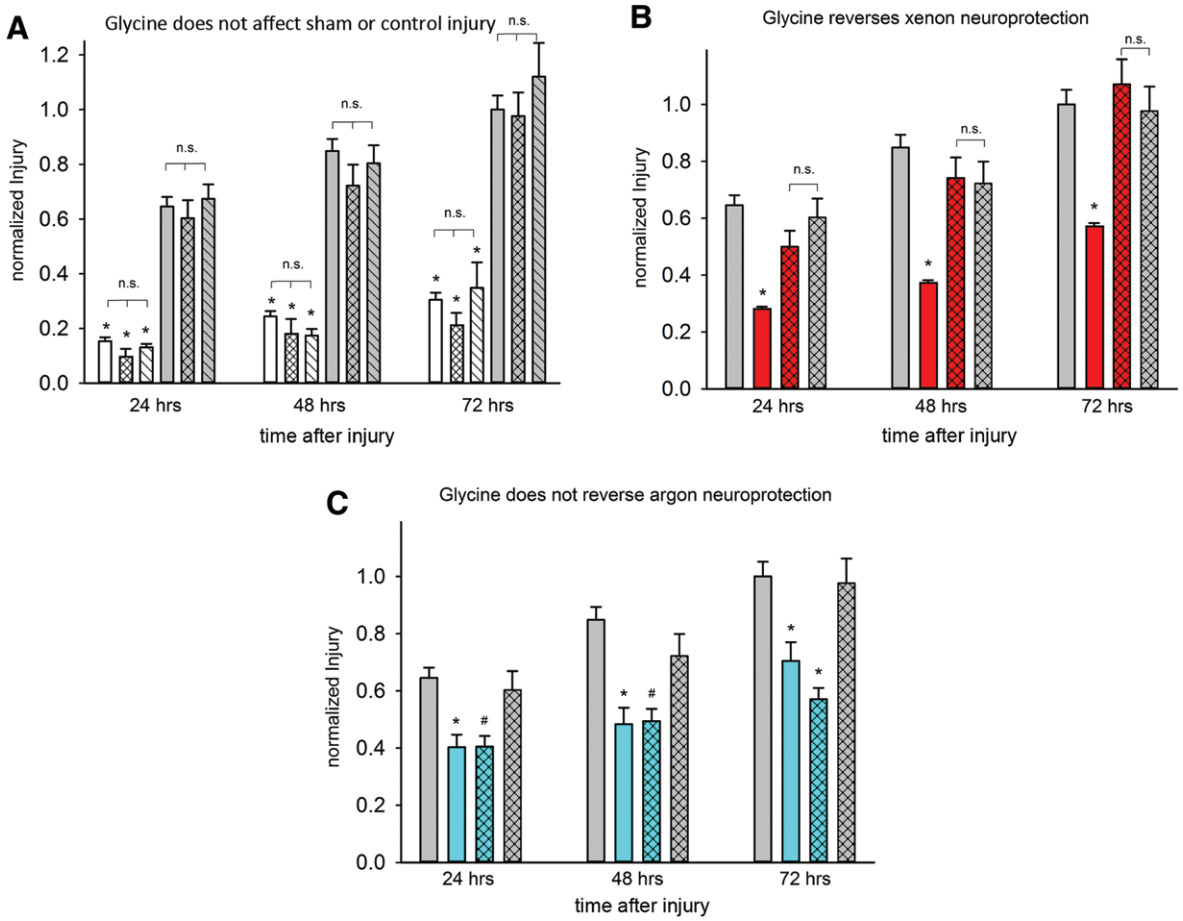


**Fig. 4.** Glycine reverses neuroprotective effect of xenon but not argon. (*A*) The addition of glycine or the inhibitory glycine receptor antagonist strychnine has no effect on injury development or sham-treated slices. Sham slices (*white bars*) were not significantly different in the presence of 100 μM glycine (*white crosshatched bars*) or 100 nM strychnine (*white hatched bars*) at any time point. Similarly, the development of control injury (*grey bars*) was not significantly different in the presence of 100 μM glycine (*grey crosshatched bars*) or 100 nM strychnine (*grey hatched bars*) at any time point. The *error bars* are standard errors (N = 141 control traumatic brain injury (TBI); N = 105 sham; N = 39 glycine TBI; N = 35 glycine sham; N = 18 strychnine TBI; N = 19 strychnine sham). (*B*) Glycine reverses the neuroprotective effect of 50% xenon. In the absence of glycine, 50% xenon (*red bars*) protects against trauma (*grey bars*). The addition of 100 μM glycine abolishes the protective effect of 50% xenon. In the presence of glycine, there was no significant difference between injured slices in the absence (*grey crosshatched bars*) or presence of xenon (*red crosshatched bars*) at any time point. The *error bars* are standard errors (N = 141 TBI; N = 104 xenon; N = 32 xenon glycine; N = 39 glycine TBI). (*C*) Glycine does not reverse the neuroprotective effect of 50% argon. In the absence of glycine, 50% argon (*cyan bars*) protects against trauma (*grey bars*). In the presence of 100 μM glycine, 50% argon (*cyan crosshatched bars*) retains a protective effect compared with injured slices (*crosshatched grey bars*). The *error bars* are standard errors. (N = 141 TBI; N = 44 argon; N = 37 argon glycine; N = 39 glycine TBI). *Indicates value significantly different ($P < 0.001$) from the control injury at each time point. #Indicates value significantly different ($P < 0.05$) from control injury at each time point.

affect the magnitude of the traumatic injury or its development over time, we investigated the effect of glycine on the neuroprotective effect of xenon. Figure 4B shows that in the absence of added glycine, 50% atm xenon had a significant neuroprotective effect, reducing injury to 43 ± 3%, 44 ± 3%, and 57 ± 3%, of nontreated injured slices at 24, 48, and 72 h after injury ($P < 0.001$). The addition of 100 μM glycine abolished xenon's neuroprotective effect. At all time points, in the presence of glycine, the xenon-treated injured slices were not significantly different to the untreated injury controls (fig. 4B), being 82 ± 9% ($P > 0.2$), 103 ± 11% ($P > 0.8$), and 113 ± 14% ($P > 0.3$) of the control at 24, 48, and 72 h after injury. A powerful feature of our model is that at each time point, glycine reversed the effect of xenon to the level of the untreated slices at the same time point. Taken together with the lack of effect of glycine on the control injury, this means that the effect of glycine cannot be explained by an exacerbation of the injury. The reversal of xenon's protective effect is consistent with xenon neuroprotection against traumatic injury being mediated by xenon inhibition at the NMDA receptor glycine site.

Because argon had a similar, although lesser, neuroprotective effect to xenon, we investigated the effect of glycine on argon neuroprotection, to determine whether argon and

xenon act *via* a similar mechanism. Interestingly, as shown in figure 4C, we found that glycine did not reverse the neuroprotective effect of argon, in contrast with its effect on xenon neuroprotection. In the presence of 100 μM glycine, 50% atm argon treatment resulted in significant neuroprotection ($P < 0.05$) at all time points. There was no difference in argon-treated slices in the absence or presence of glycine at 24, 48, and 72 h. This is not consistent with argon's protective effect being mediated *via* the NMDA receptor glycine site and indicates that argon has a different mode of action to xenon.

### Electrophysiology

To further investigate the mechanism of argon neuroprotection, we determined whether argon, and the other inert gases, had an effect on NMDA receptors and TREK-1 channels expressed in HEK-293 cells (fig. 5). Figure 5A shows electrophysiological recordings from GluN1/GluN2A NMDA receptors in the absence and presence of argon. Argon (80%) had no effect on NMDA receptor–mediated currents, at either high (100 μM) or low (1 μM) glycine concentrations, in contrast to xenon, which inhibits NMDA receptors, as we have previously shown.[34,36,38,43] Krypton, neon, and helium were also without effect on NMDA receptors as shown in figure 5B. Having ruled out NMDA receptor inhibition as a mechanism of argon neuroprotection, we determined whether argon and the other inert gases activated TREK-1 potassium channels. Untransfected cells passed only a few picoamperes or less when clamped at −50 mV (N = 3 data not shown). In contrast, cells expressing TREK-1 channels exhibited a characteristic large outwardly rectifying current that reversed at −80 mV. We used halothane as a positive control to activate TREK-1 currents; 0.82 mM halothane potentiated TREK-1 currents by 152 ± 20% (N = 10; data not shown). Figure 5C shows recordings from HEK cells expressing TREK-1 channels in the presence and absence of argon. Argon (80%) had no effect on TREK-1 currents. We found that krypton, neon, and helium were also without effect on TREK-1 (fig. 5, D–F and H). In contrast to the other inert gases, xenon (80%) activated TREK-1 currents markedly (fig. 5G), potentiating the current measured at −50 mV by 39 ± 5%, as shown in figure 5H.

## Discussion

We investigated the neuroprotective mechanisms of the noble gases such as helium, krypton, neon, argon, and xenon in an *in vitro* model of TBI. Cultured hippocampal mouse brain slices were subjected to a reproducible mechanical trauma, and injury was quantified by PI fluorescence. Organotypic cultures retain a heterogeneous population of cell types whose synaptic connectivity mirrors that seen *in vivo*,[45–49] and are intermediate between dissociated cell cultures and whole-animal models. The reproducibility of the primary focal trauma, and the progressively developing secondary injury (fig. 1), provides a useful model in which to investigate the efficacy and mechanism of putative treatments.[19,40,50,51] This *in vitro* model allows us to control the slice environment, particularly the concentration of glycine. Although the PI fluorescence measure of injury in this model does not distinguish between cell types (*e.g.*, neuronal and nonneuronal cells), it has the advantage of providing a robust quantification of traumatic injury, allowing continuous monitoring of the same slices over time.

Within 30 min of mechanical injury, PI fluorescence was evident, allowing clear distinction from uninjured slices (fig. 1). Secondary injury developed rapidly in the hours after trauma. One hour after injury, the lesion had developed to 32 ± 4% and by 6 h to 51 ± 8% of its extent at 72 h after injury. This secondary injury, developing rapidly in the hours and more slowly in the days after trauma, mirrors what is seen *in vivo*[52] and in clinical traumatic injury progression.[53,54] We measured cell death and neuroprotection in the hippocampal slice as a whole, avoiding subjective difficulties associated with precisely defining the boundaries of CA1, CA3, and dentate gyrus in each slice. Although some areas, such as CA1, appear to be more sensitive to traumatic injury (fig. 1A), qualitatively xenon and argon protected equally in different areas (data not shown), in line with studies regarding ischemic injury showing little regional differences in neuroprotection.[34,55–57]

### Effect of Noble Gases on Traumatic Injury

An aim of our study was to evaluate the neuroprotective potential of the series of noble gases against traumatic injury under identical conditions. We found that only xenon and argon exhibited neuroprotection (fig. 2). The lack of effect of 50% atm helium (fig. 1D) on traumatic injury in this model is similar to what we found using the same organotypic preparation in a model of ischemic injury.[34] Neon and krypton were also devoid of a protective effect. Xenon was particularly effective, with 50% atm xenon reducing total injury by 57% at 24 h after injury and by 43% at 72 h after injury. The degree of protection against total injury that we observed with 50% xenon was similar to that found by Coburn *et al.*[19] who used 75% xenon. Argon was less effective than xenon, with 50% atm argon reducing total injury by 38% at 24 h after injury and by 30% at 72 h after injury. This contrasts with the findings by Loetscher *et al.*[28] who reported approximately 80% reduction in injury by 50% argon in an *in vitro* trauma model, but the reason for the difference is not clear.

Xenon strongly inhibited the development of secondary injury (fig. 3A), with 50% atm xenon preventing secondary injury development at 24 and 48 h after trauma. Our finding that xenon completely arrests secondary injury at 24 and 48 h after trauma is novel and is particularly relevant to xenon's potential clinical use because clinical lesions may develop significantly in the first 24 h after injury.[53,54] The reason why xenon appears slightly less effective at 72 h is unclear, but it may reflect the fact that additional injury is occurring (*e.g.*, due to exhaustion of nutrients in the culture

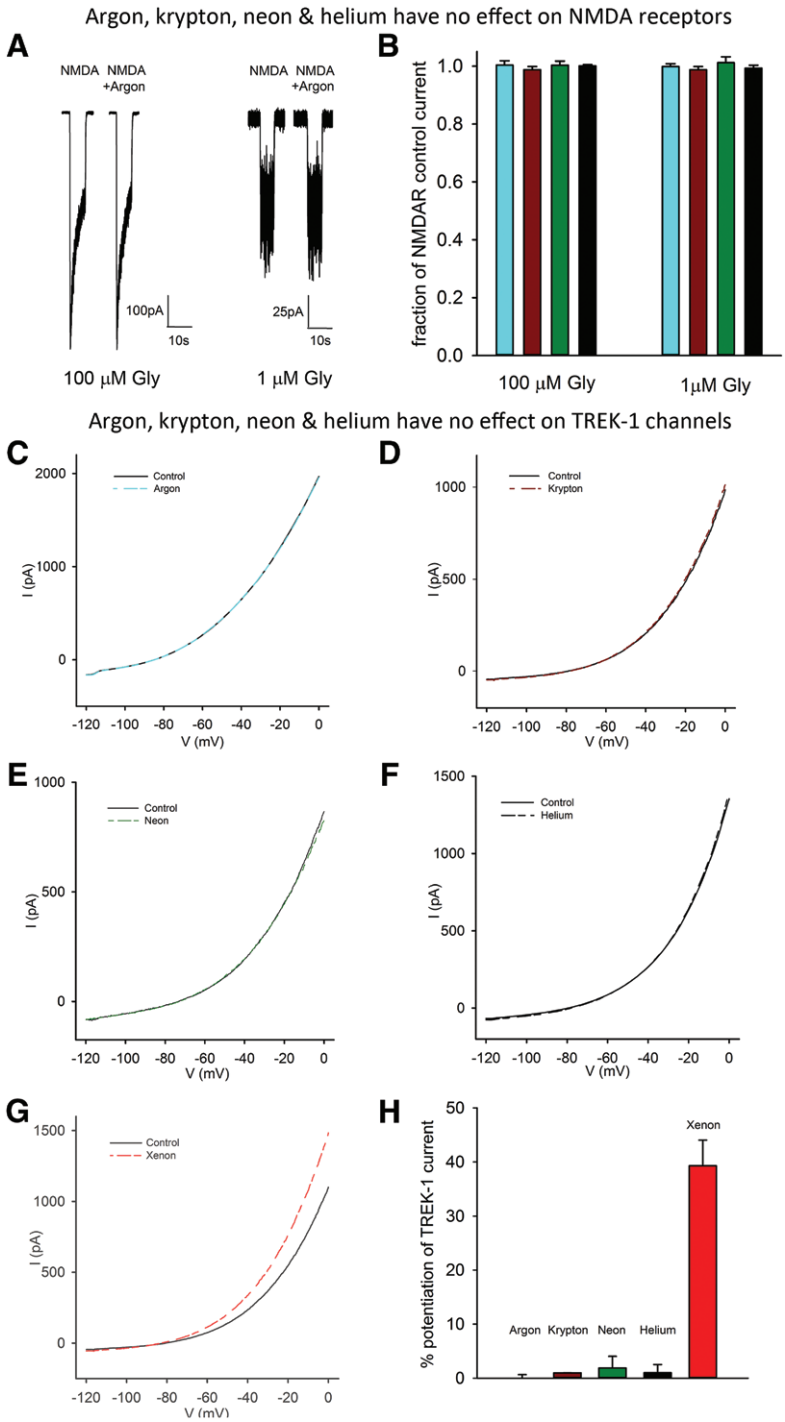


**Fig. 5.** Inert gases such as argon, krypton, neon, and helium have no effect on *N*-methyl-D-aspatate (NMDA) receptors and TREK-1 channels. (*A*) Argon (80%) has no effect on NMDA-activated currents at high glycine (100 μM) and low glycine (1 μM) concentrations. Traces show typical currents activated by 100 μM NMDA in HEK cells expressing NMDA receptors containing the GluN1/GluN2A subunit combination. (*B*) NMDA receptor currents were unaffected by 80% argon (*cyan bars*), 80% krypton (*brown bars*), 80% neon (*green bars*), or 80% helium (*black bars*). The *error bars* are standard errors (100 μM glycine: argon N = 10, krypton N = 9, neon N = 5, helium N = 9; 1 μM glycine: argon N = 12, krypton N = 9, neon N = 6, helium N = 6). (*C–F*) Inert gases argon (80%), krypton (80%), neon (80%), and helium (80%) have no effect on TREK-1 potassium channel currents. (*G*) Xenon (80%) activates TREK-1 potassium channel currents. Data were sampled at 20 kHz and each trace contains 3,000 data points, *lines* shown are through these individual points. (*H*) Xenon (*red bar*) potentiates TREK-1 currents by 39 ± 5%, whereas argon (*cyan bar*), krypton (*brown bar*), neon (*green bar*), and helium (*black bar*) do not potentiate TREK-1 currents, measured at –50 mV. The *error bars* are standard errors and where not shown they are smaller than the bar (xenon, N = 5; argon, N = 3; krypton, N = 9; neon, N = 4; helium, N = 3).

media) against which xenon is less effective. Argon attenuated the development of secondary injury at all time points, but was less effective than xenon (fig. 3B). Secondary injury in argon-treated slices was reduced but not prevented, with a maximum reduction of 51 ± 7% at 48 h after injury.

The degree of protection against secondary injury that we observed with xenon and, to a lesser extent, argon is notable, given that in our protocol the noble gas is present only *after* the insult, unlike some models where the neuroprotectant is also present before, during, and after the insult. Our protocol ensures that the insult itself remains a constant, and that any neuroprotection cannot be explained simply by an attenuation of the primary insult. This more closely models the clinical scenario when a patient presents for treatment after the traumatic injury. The fact that under identical conditions, helium, neon, and krypton were found to have no effect indicates that these gases are without neuroprotective effect in this model. The lack of effect of helium, neon, and krypton on NMDA receptors and TREK-1 channels (fig. 5) is consistent with their lack of neuroprotective effect.

### Reversal of Xenon Neuroprotection by Glycine

Our strategy to determine whether xenon neuroprotection was mediated by inhibition of the NMDA receptor at its glycine-binding site was based on our observation that xenon competes with glycine, and that xenon inhibition of the NMDA receptor is reduced at high glycine concentrations.[37] We investigated whether the degree of neuroprotection in our *in vitro* model could be modulated by altering the glycine concentration. We have previously validated this approach in a model of ischemic injury.[34] We showed that adding a saturating concentration of glycine had no effect on the control injury or on sham-treated slices (fig. 4A), but that adding glycine abolished xenon neuroprotection completely at all time points (fig. 4B). These results are consistent with xenon neuroprotection against traumatic injury being mediated by inhibition of the NMDA receptor at its glycine site. This finding is important because it clearly identifies the NMDA receptor as a target mediating xenon neuroprotection against traumatic injury. Estimates of normal brain extracellular glycine concentrations, from microdialysis experiments, are approximately 5 μM,[58,59] at which concentration xenon will inhibit NMDA receptors. Glutamate excitotoxicity is involved in neuropathologies such as ischemia and TBI.[11,13] Hence, xenon's inhibition of NMDA receptors is plausible as a mechanism of neuroprotection. However, it has become clear that there are other potential targets for xenon neuroprotection that are as plausible as the NMDA receptor. For example, the two-pore domain potassium channel TREK-1 is activated by xenon (fig. 5 and see study by Gruss [42]). That TREK-1 activation may have a role in ischemic injury is suggested by the finding that genetic ablation of TREK-1 increases sensitivity to ischemia and epilepsy in *in vivo* models.[60] Whether activation of these TREK-1 channels play a role in xenon neuroprotection against TBI remains to be determined. However, our current findings indicate that xenon neuroprotection in our model of traumatic injury can largely be accounted for by xenon inhibition of the NMDA receptor at its glycine-binding site.

### Mechanism of Argon Neuroprotection against TBI

Despite growing evidence that argon is neuroprotective,[27–29,31,35] there have been few studies that have investigated mechanisms for argon's biological actions. Our finding that argon neuroprotection is not reversed by glycine indicates that argon's neuroprotective effect is not mediated by the NMDA receptor glycine site. This is supported by our electrophysiological results showing that argon has no effect on NMDA receptors at high or low glycine concentrations (fig. 5, A and B). The lack of effect of argon on TREK-1 currents (fig. 5, C and H) indicates that this potassium channel is not involved in argon neuroprotection. The molecular mechanism(s) by which argon exerts its neuroprotective effects merits further investigation. A recent study by Fahlenkamp *et al.*[61] found that argon transiently increased levels of phosphorylated extracellular signaling kinase 1/2 *in vitro*, but whether this is involved in argon neuroprotection remains to be determined.

### Relevance to Use of Inert Gases as Neuroprotectants

We have shown that both xenon and argon protect against TBI in an *in vitro* model, and we demonstrate that xenon's neuroprotective effect is largely mediated by inhibition at the NMDA receptor glycine site. Our findings indicate that both these inert gases merit further investigation as neuroprotectants in *in vivo* models of trauma. In the case of xenon, the identification of the mechanism(s) is particularly relevant to clinical studies. We have shown that xenon acts at two targets likely to play a role in neuroprotection, namely NMDA receptors and TREK-1 channels.[7,26] It may be that the reason xenon is particularly effective as a neuroprotectant is its action at both these targets. Such a pleiotropic mechanism has been suggested to underlie neuroprotection by other anesthetic agents.[6,62,63] In addition, drugs that act at the glycine site of the NMDA receptor (*e.g.*, gavestinel) are well tolerated in patients and devoid of psychotomimetic side effects.[64] Xenon is particularly attractive as a neuroprotectant because it rapidly crosses the blood–brain barrier, exhibits cardiovascular stability, and cannot be metabolized.[65–67] If xenon is shown to be neuroprotective *in vivo*, it could provide a realistic first-line treatment for brain trauma patients.

The authors thank Raquel Yustos, M.Sc., Research Technician, Biophysics Section, Imperial College London, London, United Kingdom, for technical support; Dr. Valeria Bridi, M.D., Medical Student, University of Pavia, Pavia, Italy, for help building the trauma device; and Paul Brown, Workshop Manager, and Steve Norris, Workshop Technician, Physics Department, Imperial College London, London, United Kingdom, for their help in building the xenon chamber.

## References

1. Bruns J Jr, Hauser WA: The epidemiology of traumatic brain injury: A review. Epilepsia 2003; 44(suppl 10):2–10

2. Langlois JA, Rutland-Brown W, Wald MM: The epidemiology and impact of traumatic brain injury: A brief overview. J Head Trauma Rehabil 2006; 21:375–8
3. Tolias CM, Bullock MR: Critical appraisal of neuroprotection trials in head injury: What have we learned? NeuroRx 2004; 1:71–9
4. Wang KK, Larner SF, Robinson G, Hayes RL: Neuroprotection targets after traumatic brain injury. Curr Opin Neurol 2006; 19:514–9
5. Warner DS, Borel CO: Treatment of traumatic brain injury: One size does not fit all. Anesth Analg 2004; 99:1208–10
6. Greve MW, Zink BJ: Pathophysiology of traumatic brain injury. Mt Sinai J Med 2009; 76:97–104
7. Ling GS, Marshall SA: Management of traumatic brain injury in the intensive care unit. Neurol Clin 2008; 26:409–26, viii
8. Loane DJ, Faden AI: Neuroprotection for traumatic brain injury: Translational challenges and emerging therapeutic strategies. Trends Pharmacol Sci 2010; 31:596–604
9. Raghupathi R: Cell death mechanisms following traumatic brain injury. Brain Pathol 2004; 14:215–22
10. Teasdale GM, Graham DI: Craniocerebral trauma: Protection and retrieval of the neuronal population after injury. Neurosurgery 1998; 43:723–37; discussion 737–8
11. Bullock R, Zauner A, Myseros JS, Marmarou A, Woodward JJ Young HF: Evidence for prolonged release of excitatory amino acids in severe human head trauma: Relationship to clinical events. Ann N Y Acad Sci 1995; 765:290–7
12. Kochanek PM, Clark RS, Ruppel RA, Adelson PD, Bell MJ, Whalen MJ, Robertson CL, Satchell MA, Seidberg NA, Marion DW, Jenkins LW: Biochemical, cellular, and molecular mechanisms in the evolution of secondary damage after severe traumatic brain injury in infants and children: Lessons learned from the bedside. Pediatr Crit Care Med 2000; 1:4–19
13. Nilsson P, Hillered L, Pontén U, Ungerstedt U: Changes in cortical extracellular levels of energy-related metabolites and amino acids following concussive brain injury in rats. J Cereb Blood Flow Metab 1990; 10:631–7
14. Wilhelm S, Ma D, Maze M, Franks NP: Effects of xenon on *in vitro* and *in vivo* models of neuronal injury. Anesthesiology 2002; 96:1485–91
15. Ma D, Wilhelm S, Maze M, Franks NP: Neuroprotective and neurotoxic properties of the 'inert' gas, xenon. Br J Anaesth 2002; 89:739–46
16. Banks P, Franks NP, Dickinson R: Xenon neuroprotection against hypoxia-ischaemia is mediated by the *N*-methyl-D-aspartate receptor glycine site. Br J Anaesth 2010; 104:526
17. Dingley J, Tooley J, Porter H, Thoresen M: Xenon provides short-term neuroprotection in neonatal rats when administered after hypoxia-ischemia. Stroke 2006; 37:501–6
18. Fries M, Nolte KW, Coburn M, Rex S, Timper A, Kottmann K, Siepmann K, Häusler M, Weis J, Rossaint R: Xenon reduces neurohistopathological damage and improves the early neurological deficit after cardiac arrest in pigs. Crit Care Med 2008; 36:2420–6
19. Coburn M, Maze M, Franks NP: The neuroprotective effects of xenon and helium in an *in vitro* model of traumatic brain injury. Crit Care Med 2008; 36:588–95
20. Ma D, Hossain M, Chow A, Arshad M, Battson RM, Sanders RD, Mehmet H, Edwards AD, Franks NP, Maze M: Xenon and hypothermia combine to provide neuroprotection from neonatal asphyxia. Ann Neurol 2005; 58:182–93
21. Homi HM, Yokoo N, Ma D, Warner DS, Franks NP, Maze M, Grocott HP: The neuroprotective effect of xenon administration during transient middle cerebral artery occlusion in mice. Anesthesiology 2003; 99:876–81
22. Sheng SP, Lei B, James ML, Lascola CD, Venkatraman TN, Jung JY, Maze M, Franks NP, Pearlstein RD, Sheng H, Warner DS: Xenon neuroprotection in experimental stroke: Interactions with hypothermia and intracerebral hemorrhage. Anesthesiology 2012; 117:1262–75
23. Bickler PE, Warren DE, Clark JP, Gabatto P, Gregersen M, Brosnan H: Anesthetic protection of neurons injured by hypothermia and rewarming: Roles of intracellular $Ca^{2+}$ and excitotoxicity. Anesthesiology 2012; 117:280–92
24. Preckel B, Weber NC, Sanders RD, Maze M, Schlack W: Molecular mechanisms transducing the anesthetic, analgesic, and organ-protective actions of xenon. Anesthesiology 2006; 105:187–97
25. Oei GT, Weber NC, Hollmann MW, Preckel B: Cellular effects of helium in different organs. Anesthesiology 2010; 112:1503–10
26. Dickinson R, Franks NP: Bench-to-bedside review: Molecular pharmacology and clinical use of inert gases in anesthesia and neuroprotection. Crit Care 2010; 14:229
27. Ryang YM, Fahlenkamp AV, Rossaint R, Wesp D, Loetscher PD, Beyer C, Coburn M: Neuroprotective effects of argon in an *in vivo* model of transient middle cerebral artery occlusion in rats. Crit Care Med 2011; 39:1448–53
28. Loetscher PD, Rossaint J, Rossaint R, Weis J, Fries M, Fahlenkamp A, Ryang YM, Grottke O, Coburn M: Argon: Neuroprotection in *in vitro* models of cerebral ischemia and traumatic brain injury. Crit Care 2009; 13:R206
29. Yarin YM, Amarjargal N, Fuchs J, Haupt H, Mazurek B, Morozova SV, Gross J: Argon protects hypoxia-, cisplatin- and gentamycin-exposed hair cells in the newborn rat's organ of Corti. Hear Res 2005; 201:1–9
30. Zhuang L, Yang T, Zhao H, Fidalgo AR, Vizcaychipi MP, Sanders RD, Yu B, Takata M, Johnson MR, Ma D: The protective profile of argon, helium, and xenon in a model of neonatal asphyxia in rats. Crit Care Med 2012; 40: 1724–30
31. David HN, Haelewyn B, Degoulet M, Colomb DG Jr, Risso JJ, Abraini JH: *Ex vivo* and *in vivo* neuroprotection induced by argon when given after an excitotoxic or ischemic insult. PLoS One 2012; 7:e30934
32. David HN, Haelewyn B, Chazalviel L, Lecocq M, Degoulet M, Risso JJ, Abraini JH: Post-ischemic helium provides neuroprotection in rats subjected to middle cerebral artery occlusion-induced ischemia by producing hypothermia. J Cereb Blood Flow Metab 2009; 29:1159–65
33. Pan Y, Zhang H, VanDeripe DR, Cruz-Flores S, Panneton WM: Heliox and oxygen reduce infarct volume in a rat model of focal ischemia. Exp Neurol 2007; 205:587–90
34. Banks P, Franks NP, Dickinson R: Competitive inhibition at the glycine site of the *N*-methyl-D-aspartate receptor mediates xenon neuroprotection against hypoxia-ischemia. Anesthesiology 2010; 112:614–22
35. Jawad N, Rizvi M, Gu J, Adeyi O, Tao G, Maze M, Ma D: Neuroprotection (and lack of neuroprotection) afforded by a series of noble gases in an *in vitro* model of neuronal injury. Neurosci Lett 2009; 460:232–6
36. Franks NP, Dickinson R, de Sousa SL, Hall AC, Lieb WR: How does xenon produce anaesthesia? Nature 1998; 396:324
37. Dickinson R, Peterson BK, Banks P, Simillis C, Martin JC, Valenzuela CA, Maze M, Franks NP: Competitive inhibition at the glycine site of the *N*-methyl-D-aspartate receptor by the anesthetics xenon and isoflurane: Evidence from molecular modeling and electrophysiology. Anesthesiology 2007; 107:756–67
38. Armstrong SP, Banks PJ, McKitrick TJ, Geldart CH, Edge CJ, Babla R, Simillis C, Franks NP, Dickinson R: Identification of two mutations (F758W and F758Y) in the *N*-methyl-D-aspartate receptor glycine-binding site that selectively prevent competitive inhibition by xenon without affecting glycine binding. Anesthesiology 2012; 117:38–47
39. Stoppini L, Buchs PA, Muller D: A simple method for organotypic cultures of nervous tissue. J Neurosci Methods 1991; 37:173–82

40. Adamchik Y, Frantseva MV, Weisspapir M, Carlen PL, Perez Velazquez JL: Methods to induce primary and secondary traumatic damage in organotypic hippocampal slice cultures. Brain Res Brain Res Protoc 2000; 5:153–8
41. Macklis JD, Madison RD: Progressive incorporation of propidium iodide in cultured mouse neurons correlates with declining electrophysiological status: A fluorescence scale of membrane integrity. J Neurosci Methods 1990; 31:43–6
42. Gruss M, Bushell TJ, Bright DP, Lieb WR, Mathie A, Franks NP: Two-pore-domain K+ channels are a novel target for the anesthetic gases xenon, nitrous oxide, and cyclopropane. Mol Pharmacol 2004; 65:443–52
43. de Sousa SL, Dickinson R, Lieb WR, Franks NP: Contrasting synaptic actions of the inhalational general anesthetics isoflurane and xenon. Anesthesiology 2000; 92:1055–66
44. Downie DL, Hall AC, Lieb WR, Franks NP: Effects of inhalational general anaesthetics on native glycine receptors in rat medullary neurones and recombinant glycine receptors in Xenopus oocytes. Br J Pharmacol 1996; 118:493–502
45. Bahr BA: Long-term hippocampal slices: A model system for investigating synaptic mechanisms and pathologic processes. J Neurosci Res 1995; 42:294–305
46. Crain SM: Development of specific synaptic network functions in organotypic central nervous system (CNS) cultures: Implications for transplantation of CNS neural cells *in vivo*. Methods 1998; 16:228–38
47. Finley M, Fairman D, Liu D, Li P, Wood A, Cho S: Functional validation of adult hippocampal organotypic cultures as an *in vitro* model of brain injury. Brain Res 2004; 1001:125–32
48. Frantseva M, Perez Velazquez JL, Tonkikh A, Adamchik Y, Carlen PL: Neurotrauma/neurodegeneration and mitochondrial dysfunction. Prog Brain Res 2002; 137:171–6
49. Frantseva MV, Kokarovtseva L, Perez Velazquez JL: Ischemia-induced brain damage depends on specific gap-junctional coupling. J Cereb Blood Flow Metab 2002; 22:453–62
50. Adembri C, Bechi A, Meli E, Gramigni E, Venturi L, Moroni F, De Gaudio AR, Pellegrini-Giampietro DE: Erythropoietin attenuates post-traumatic injury in organotypic hippocampal slices. J Neurotrauma 2004; 21:1103–12
51. Morrison B III, Saatman KE, Meaney DF, McIntosh TK: *In vitro* central nervous system models of mechanically induced trauma: A review. J Neurotrauma 1998; 15:911–28
52. Turtzo LC, Budde MD, Gold EM, Lewis BK, Janes L, Yarnell A, Grunberg NE, Watson W, Frank JA: The evolution of traumatic brain injury in a rat focal contusion model. NMR Biomed 2013; 26: 468-79
53. Servadei F, Nanni A, Nasi MT, Zappi D, Vergoni G, Giuliani G, Arista A: Evolving brain lesions in the first 12 hours after head injury: Analysis of 37 comatose patients. Neurosurgery 1995; 37:899–906; discussion 906–7
54. White CL, Griffith S, Caron JL: Early progression of traumatic cerebral contusions: Characterization and risk factors. J Trauma 2009; 67:508–14; discussion 514–5
55. Gray JJ, Bickler PE, Fahlman CS, Zhan X, Schuyler JA: Isoflurane neuroprotection in hypoxic hippocampal slice cultures involves increases in intracellular $Ca^{2+}$ and mitogen-activated protein kinases. Anesthesiology 2005; 102:606–15
56. Montero M, Nielsen M, Rønn LC, Møller A, Noraberg J, Zimmer J: Neuroprotective effects of the AMPA antagonist PNQX in oxygen-glucose deprivation in mouse hippocampal slice cultures and global cerebral ischemia in gerbils. Brain Res 2007; 1177:124–35
57. Sullivan BL, Leu D, Taylor DM, Fahlman CS, Bickler PE: Isoflurane prevents delayed cell death in an organotypic slice culture model of cerebral ischemia. Anesthesiology 2002; 96:189–95
58. Berger AJ, Dieudonné S, Ascher P: Glycine uptake governs glycine site occupancy at NMDA receptors of excitatory synapses. J Neurophysiol 1998; 80:3336–40
59. Dopico JG, González-Hernández T, Pérez IM, García IG, Abril AM, Inchausti JO, Rodríguez Díaz M: Glycine release in the substantia nigra: Interaction with glutamate and GABA. Neuropharmacology 2006; 50:548–57
60. Heurteaux C, Guy N, Laigle C, Blondeau N, Duprat F, Mazzuca M, Lang-Lazdunski L, Widmann C, Zanzouri M, Romey G, Lazdunski M: TREK-1, a K+ channel involved in neuroprotection and general anesthesia. EMBO J 2004; 23:2684–95
61. Fahlenkamp AV, Rossaint R, Haase H, Al Kassam H, Ryang YM, Beyer C, Coburn M: The noble gas argon modifies extracellular signal-regulated kinase ½ signaling in neurons and glial cells. Eur J Pharmacol 2012; 674:104–11
62. Head BP, Patel P: Anesthetics and brain protection. Curr Opin Anaesthesiol 2007; 20:395–9
63. Patel P: No magic bullets: The ephemeral nature of anesthetic-mediated neuroprotection. Anesthesiology 2004; 100:1049–51
64. Dyker AG, Lees KR: Safety and tolerability of GV150526 (a glycine site antagonist at the *N*-methyl-D-aspartate receptor) in patients with acute stroke. Stroke 1999; 30:986–92
65. Sanders RD, Franks NP, Maze M: Xenon: No stranger to anaesthesia. Br J Anaesth 2003; 91:709–17
66. Hemmings HC Jr, Mantz J: Xenon and the pharmacology of fear. Anesthesiology 2008; 109:954–5
67. Preckel B, Schlack W, Heibel T, Rütten H: Xenon produces minimal haemodynamic effects in rabbits with chronically compromised left ventricular function. Br J Anaesth 2002; 88:264–9